Applied Energy 353 (2024) 121961

Contents lists available at ScienceDirect

Applied Energy

journal homepage: www.elsevier.com/locate/apenergy

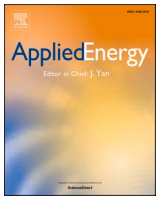

Assessing school ventilation strategies from the perspective of health, environment, and energy

Fatos Pollozhani [a,*], Robert S. McLeod [a], Christian Schwarzbauer [b], Christina J. Hopfe [a]

[a] Institute for Building Physics, Services and Construction (IBPSC), Graz University of Technology, Graz, Austria
[b] Department of Applied Sciences and Mechatronics, Hochschule München University of Applied Sciences, Munich, Germany

HIGHLIGHTS

- 5 classroom ventilation strategies were evaluated using measured and modelled data.
- Mechanical and hybrid ventilation were compared to natural ventilation strategies.
- Energy, thermal comfort, IAQ and SARS-CoV-2 infection risk criteria were evaluated.
- None of the ventilation scenarios could eliminate the risk of aerosol transmission.
- Hybrid systems provide the best compromise solution for all criteria.

ARTICLE INFO

Keywords:
Building performance simulation
Energy efficiency
Indoor air quality
Airborne transmission of SARS-CoV-2

ABSTRACT

The global COVID-19 pandemic has highlighted the importance of indoor air quality and ventilation to mitigate the spread of respiratory viral infections. Schools, in particular, represent a vulnerable environment with high occupancy rates, prolonged exposure times and often inadequately ventilated rooms. This paper evaluates the functionality of different natural and retrofitted mechanical ventilation strategies in this context. An experimental setup, combining empirical measurements with building performance simulation and analytical risk analysis was used to assess key performance characteristics, including the energetic performance, thermal comfort, indoor air quality and the airborne infection risk of SARS-CoV-2. The results of this study underscore the need for a holistic approach to ventilation design in schools, taking into consideration the balance between energy performance, carbon emissions, thermal comfort, indoor air quality and associated health factors. We demonstrate that the risk of one or more long-range airborne infections, with the SARS-CoV-2 Omicron variant, can be reduced by >50% through appropriate use of natural, mechanical or hybrid ventilation in a classroom setting. Analytical modelling demonstrates that this risk can be further reduced, by an order of magnitude, through the use of FFP2 masks.

1. Introduction

Educational institutions were highly impacted during the peaks of the SARS-CoV-2 viral pandemic [1,2]. Whilst some authors argued that the role of school transmission was no worse than elsewhere in the community [3] or needed further elucidation [4] others identified poorly ventilated classrooms a key node of transmission [5,6]. Since the beginning of 2020, various prevention strategies, including mandatory mask-wearing, large-scale testing, quarantining, and school closures accompanied by remote learning, were used to safeguard the health and safety of students and staff across educational institutions [7]. Collectively these mitigation strategies showed a marked effect in reducing infection transmission rates and safeguarding public health [8,9]. Despite this success economic impacts [10,11] including excessive inflation [12] were cited alongside socio-economic concerns [13,14], including the exacerbation of child poverty [15], as reasons to reopen schools. At the same time some authors claimed that remote learning and prophylaxis measures (such as masking) had both real [16] and perceived [17,18] negative impacts on student wellbeing, notably in relation to mental health [19] and psychological wellbeing [20]. Consequently, these measures were brought to an abrupt end in most Western societies. When schools returned to normal operation,

* Corresponding author.
E-mail address: fatos.pollozhani@tugraz.at (F. Pollozhani).

https://doi.org/10.1016/j.apenergy.2023.121961
Received 14 June 2023; Received in revised form 5 September 2023; Accepted 11 September 2023
Available online 7 October 2023

following the delta-wave, most did so without installing indoor air quality monitoring or upgrading ventilation systems, thereby removing all preventative measures [21].

The legacy of challenges highlighted by the SARS-CoV-2 pandemic [22,23] are not the only drivers for re-evaluating ventilation in schools, however. Seasonal influenza outbreaks [24,25] and the risk of future airborne pandemics [26], as well as observations of health issues from airborne contaminants and off-gassing [27,28] and impaired cognitive performance associated with poor indoor air quality [29,30], underscore the need for further measures to improve ventilation in educational institutions world-wide. Many researchers believe that greater emphasis needs to be placed on the role of heating, ventilation, and air-conditioning (HVAC) systems as a means of controlling the spread of viral diseases and improving overall IAQ [31] In particular, the role of ventilation as a means of reducing both short- [32] and long-range [33] viral aerosol transmission risks has been highlighted. In this regard, indoor CO_2 concentrations have been widely used as a proxy indicator for indoor air quality, due to the co-exhalation of CO_2 molecules and respiratory aerosols, as well as the general relationship between room-air CO_2 concentrations, occupancy, and air-exchange rates [34,35]. Moreover, several studies have used exhaled CO_2 fractions [36,37], sometimes in conjunction with numerically derived air exchange rates [38], as a means of estimating airborne SARS-CoV-2 infection transmission risks. An important distinction should be made, however, in relation to the use of CO_2 as an indicator of ventilation rates (and therein of exhaled aerosol concentrations) in contrast to its use as a general indicator of indoor air quality (IAQ). CIBSE Guide TM64 (2020) [39] and a number of IAQ studies carried out in schools [40,41] have emphasised the need to consider multiple indicators (including moisture, particulates, VOCs and a wide range of other contaminants) in addition to CO_2, in order to provide a broader assessment of IAQ.

European standard EN 16798–1:2019 [42], and international standard ISO 17772-1:2017 [43] define appropriate ventilation rates and target CO_2 levels applicable to school buildings, wherein 550 ppm above ambient (i.e. circa 980 ppm) represents the limiting threshold value for category IEQ_I indoor environmental conditions (which are considered suitable for children and occupants with special needs [[42], p. 18]). It is notable however, that these standards were formulated prior to the SARS-CoV-2 pandemic. In the context of the SARS-CoV-2 pandemic European building services organisation such as CIBSE and REHVA have advocated the use of CO_2 sensors with the aim of ensuring that ventilation is sufficient to maintain CO_2 concentrations below 800 ppm [44,45] and not to exceed 1000 ppm [46]. In response to the removal of mask mandates and the increased contagiousness of the Omicron variants Rowe et al. recommended 800 ppm as a suitable limiting threshold, whilst wearing a mask, and 600 ppm without a mask [47]. A distinction should be made here in relation to short-range (droplet) and long-range (droplet nuclei) [48] transmission of SARS-CoV-2 and other airborne viruses. Whilst most airborne infection risk models attempt to capture the relative risk of time-weighted exposure to room-air containing well mixed aerosols, they are unable to account for short-range (droplet) transmission. It has been generally accepted that respiratory droplets, released through speaking, singing, or coughing can travel a short-distance (i.e. 1–2 m) from an infectious person, although studies have also shown that whilst sneezing such droplets may reach distances of up to 8 m [49]. Regardless of whether the droplet or aerosol modality dominates short-range transmission [50], occupant density and the spacing of rows of desks (and lecture theatre seating plans) are important considerations when considering risk mitigation in educational settings [51].

Several large-scale cohort studies have now provided relevant insights into the contribution of ventilation in relation to airborne infection transmission risks in European schools. Studies in >240 classrooms in Germany, over an entire school year, found that the percentage of overall teaching time in which a CO_2 value of 1000 ppm was exceeded amounted to 24% with natural window ventilation and 21% with a central mechanical ventilation system [52]. Significant improvements were achieved by installing fan-assisted window ventilation and decentralized ventilation systems, with 16% and 11% of the teaching time, respectively, showing CO_2 values above 1000 ppm [52]. In Switzerland, correlations between poorly ventilated classrooms and increased SARS-CoV-2 infection rates, were demonstrated in 150 classrooms [53]. Meanwhile, in over 1400 Italian schools, it was shown that mechanical ventilation systems were able to reduce the relative risk of students becoming infected, with SARS-CoV-2, by approximately 80%, at a ventilation rate of >10 L/s (per person), compared to classrooms reliant upon natural ventilation [54].

Whilst the added benefits of further reducing pathogenic aerosol concentrations are clear, the implications of setting lower CO_2 targets as a means of achieving this goal need to be considered in a wider context. When proposing new IAQ targets and ventilation strategies for schools' complex global issues such as the energy and climate crises need to be addressed alongside the need to maintain acceptable levels of thermal comfort, whilst safeguarding health, wellbeing, and academic attainment.

Based on the challenges posed by this multi-faceted context this study assesses the trade-offs between five alternative (natural, mechanical and hybrid) ventilation strategies in relation to four key performance indicators (ventilation rate, SARS-CoV-2 infection risk, energy consumption and thermal comfort) in the context of a European university seminar room.

2. Methods

In the first phase of this study, a seminar room at Graz University of Technology was equipped with a novel retrofitted mechanical extract ventilation (MEV) system developed by the Max Planck Institute for Chemistry (MPIC), Germany, as a means of minimising the risk of SARS-CoV-2 transmission in naturally ventilated classrooms [55,56] (see Section 2.1 and Appendix A1 for more information). Ventilation air flow measurements, air infiltration tests and room Indoor Environmental Quality (IEQ) monitoring were then conducted on the assembled system (see Section 2.3). Building performance simulations (BPS) were then carried out, using empirical data from the experimental setup, in order to generate key performance data across an entire year of operation. Four further ventilation scenarios (involving natural, mechanical and hybrid ventilation systems) were then investigated using the validated IDA ICE dynamic simulation software (see Section 2.2). Finally, the infection risk associated with the various scenarios was analytically assessed based on a method developed by Lelieveld et al. [57] (see Section 2.4).

2.1. Experimental setup

The room selected for this study is characteristic of many naturally ventilated university seminar rooms, designed for approximately 30 occupants. The room is typically used from 8 a.m. to 5 p.m. for various purposes including lectures, workshops, and exams. Thus the room occupancy will vary over the course of a day and also seasonally, and for this reason a range of occupancy levels (n = 10, 20 and 30) were investigated in this study.

The seminar room was located on the first floor of a five-storey university building constructed in 1994. For the purpose of creating an accurate BPS model the dimensions of the building were taken from existing plans. Fig. 1 shows the floor plan of the seminar room with the MPIC-MEV system overlaid. With rectangular proportions and internal dimensions of 6.5 by 8.1 m and a height of 3.05 m (minus three vertical columns) the room had a net internal volume of 147.3 m^3. One of the four walls was an exterior wall facing southwest. Five openable (tilt and turn) windows measuring 0.9 by 1.8 m resulted in a window-to-wall ratio of 33% (8.1 m^2 of 24.7 m^2 interior wall). The windows were equipped with external horizontal fixed-angle louvers for sun

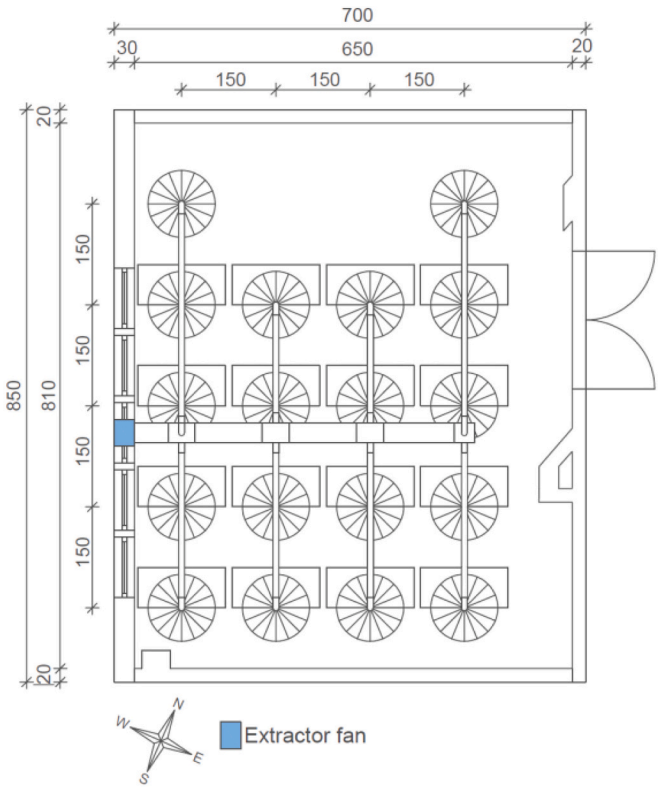

Fig. 1. Floor plan of the seminar room showing the layout of the MPIC-MEV system.

protection, which covered approximately half of the windows' aperture.

Heating to the room was generated centrally by a district heating system and distributed to the room through two wall mounted radiators (1.4 m by 0.5 m) with an estimated design power output of 2350 W each. The radiator temperatures were individually controlled by self-regulating thermostatic radiator valves (TRVs). The seminar room was illuminated with 16 compact fluorescent lamps with an electric power consumption of 25 W each (400 W in total, with a 30% convective heat fraction). In addition, a ceiling mounted projector with a power consumption of 150 W was installed in the room. Resulting in a total internal heat gain of 550 W for lights and equipment. The thermal performance of the construction materials was taken from an energy certificate issued in 2012. Table 1 shows the thermal properties of the construction materials and the corresponding U-values.

An average infiltration rate of 0.2 h^{-1} was determined for the room, using measurements taken over an eight-day period. This figure was derived from concentration decays of human-generated CO_2 in the space using the approach described by Persily [58], Turiel and Rudy [59] and Cui et al. [60] (this calculation can be found in Appendix A2).

For the purpose of this study, this naturally ventilated university seminar room was equipped with the MPIC-MEV system (for more information and images of the ventilation system see Appendix A1). This uses a lightweight duct system connected to an array of extract hoods positioned above the desks to extract the stale indoor air to the outside. The system is designed to extract stale room-air close to the ceiling and supply fresh air nearer to the floor level, through a tilted window. This means that the system utilizes the vertical stratification of indoor air and heat plumes generated by occupants to directly capture and remove respiratory aerosols before they are mixed into the ambient air [56]. The displacement effect has been shown to improve the air quality in the breathing zone of seated occupants by up to 50% [61]. In the context of COVID-19, it has been observed that displacement ventilation provides the most effective means of mitigating the risk of long-range transmission, if properly designed, since it minimises the mixing of room air and promotes the vertical stratification of warm stale air [62,63].

Table 1
Thermal properties of construction materials.

Structural components	U-Value [W/m^{2}K]
Exterior wall	0.34
Windows (U_w)	2.00
Interior walls	1.01
Interior floors/ ceilings	0.79

2.2. Building simulation and scenarios

In this study the BPS software IDA ICE 4.8 (2020) [64] was used to perform dynamic simulations to evaluate the MPIC-MEV system's energetic performance as well as the resultant indoor climate. The IDA ICE software has been validated according to ASHRAE 140–2004 [65], CIBSE TM 33 [66], EN 15255–2007 and EN 15265–2007 [67]. A digital building model of the seminar room was created, based upon the real building's dimensions, HVAC systems, lights, external sun protection and components. The simulations were carried out for three different occupant densities (n = 10, 20 and 30 people). In order to reflect the long-term mean climatic conditions in this location a reference year weather file was generated using the Meteonorm (version 7.2) software [68]. The reference year used in this study was taken from measurements at the weather station Graz Thalerhof, which is located approximately 10 km from the considered building. The weather file contained 12 months of hourly data compiled to represent the mean external environment of a long-term observation period (from 1991 to 2019). The data was interpolated (using Meteonorm 7.2 software [68]) to the precise location of the university building, in order to take into account urban heat island effects. The software uses a 3-D inverse distance model (Shepard's gravity interpolation) to calculate meteorological data for any chosen location [69,70]. This method is based on the assumption that the attributes of two (or more) interpolation points are related, and that their influence is inversely proportional to the distance between them [71], similar interpolation approaches have been adopted in other studies [72,73] in order to more accurately model the localised effects of the urban microclimate. A number of different scenarios were simulated in order to investigate how different ventilation approaches (including natural ventilation strategies) affected the energetic performance, carbon emissions, indoor climate, and infection risk. The five ventilation scenarios (S1-S5) considered are described hereafter and summarised in Table 2.

1. Base Case (BC)

The base case (BC) assumed a seminar room in which no purposeful ventilation measures were taken (i.e. all windows and doors remained closed). The main purpose of this scenario was to serve as a worst-case comparator for the IAQ and infection risk, and as a best-case scenario for heating energy conservation. It should be noted, that whilst empirical data shows that such a scenario is not uncommon, it would not comply with European ventilation standard EN 16798–1 [42] (or any international IAQ standard) and its use as a ventilation strategy is therefore not advised.

2. Max Planck Institute for Chemistry–Mechanical Extract Ventilation (MPIC-MEV)

The second scenario examined the MPIC–MEV system (as described in Appendix A1) installed in the seminar room. The air exchange rates were measured directly from the installed system along with the influence of the control mechanisms implemented in the simulation (see Section 3.1 for the measured air flow rates and control mechanisms).

Table 2
List of considered scenarios and simulation parameters.

Parameters	1. BC	2. MPIC-MEV	3. AHU-HRV	4. NV-T	5. NV-P
Air flow [L/s(m^2)]	0.17[a]	2.90/4.45[b]	2.90/4.45[b]	variable [c]	variable[c]
Occupancy schedule [d e]			8 a.m.–12 p.m., 1 p.m.–5 p.m.		
Fan, window, equipm. sched.			8 a.m.–12 p.m., 1 p.m.–5 p.m.		
Fan set-back schedule [f]	–	–	7 a.m.-8 a.m. 12 p.m.-1 p.m.	–	–
Number of open windows[g]	–	1 tilted	–	5 tilted	5 fully open
Fan energy cons. [W]	–	47 / 71[h]	374	–	–
HX thermal efficiency [%]	–	–	81	–	–
Active internal heat gains			100% of internal gains due to occupants, equipment, light		
Radiator design power [W]			2 × 2350		
Temperature setpoint [°C]			20 °C (using a 2 °C P-band for proportional temperature control)		

[a] Value achieved solely by infiltration, which is not considered purposeful ventilation.
[b] See Section 3.1 for the occupancy dependent ventilation control strategies used in scenarios 2 and 3.
[c] 'variable' because values were determined by IDA ICE tool for transient external/ internal boundary conditions.
[d] Metabolic rate of 126 W (sensible and latent heat, at 1.2 met and 70 W/m^2) acc. to ISO 7730:2005 [74].
[e] Weekends and holidays (acc. to Austrian university curriculum, i.e. Feb., Jul., Aug., Sept.) lecture free.
[f] Set-back rate of one volumetric air change within two hours prior to occupancy (0.5 h^{-1}) acc. to EN 16798–1:2019 [42].
[g] Total free opening area of 0.5 m^2 per tilted window and 1.8 m^2 per fully open window.
[h] The power consumption of 47 W at 2.90 L/s(m^2) and 71 W at 4.45 L/s(m^2) was measured on the installed system.

3. Air Handling Unit – Heat Recovery (AHU-HRV)

In the third scenario, a conventional decentralized air handling unit (AHU) with heat recovery (HRV) was used. An AHU with a nominal air flow rate of 0.2 m^3/s (i.e. 720 m^3/h, at a nominal external pressure of 200 Pa) was chosen for the simulation [76] as this approximately corresponded to the air flow rates measured on the MPIC-MEV system in scenario 2. Based on a single node room air model (IDA ICE v4.8) the supply and exhaust air are assumed to be homogeneously distributed in the room with predefined air flow rates depending on the occupant density (see Section 3.1 for ventilation rates). During warmer periods the HR system was operated in bypass mode. Thus, when the outside air temperature exceeded 16 °C the extract air was discharged through the bypass (avoiding the heat exchanger) in order to prevent unwanted heat recovery, which might exacerbate overheating at this time.

4. Natural Ventilation – Tilted windows (NV-T)

Scenario 4 examined the ventilation of the seminar room by the means of tilted windows. For this case, it was assumed that all five windows of the room were continuously tilted (with a maximum opening depth of 0.18 m, providing a total window opening area of 0.5 m^2 per window, calculated according to Mourkos et al. [77]) during occupied periods (i.e., from 8 a.m. till 12 p.m. and from 1 p.m. till 5 p.m.). This scenario was designed to reflect the background ventilation which would occur through the use of constantly tilted windows, without requiring additional occupant intervention.

5. Natural Ventilation – Purge ventilation (NV-P)

Scenario 5 investigated purge ventilation patterns using fully opened windows. This strategy was advocated by the German environmental agency (German: Umweltbundesamt, UBA) at the outbreak of the pandemic. UBA recommended that classrooms should be purge ventilated at regular intervals, using wide-open windows instead of tilted windows [78]. In this scenario it was defined that all five windows of the seminar room were fully opened every 20 min for a duration of 4 min during the months of October through to April. In the months of May and June, when the average daily temperatures were around 17 to 20 degrees Celsius, the windows were opened for an extended period, of 15 min, every 20 min to compensate for the reduced air- pressure differentials occurring between the inside and outside air masses at this time.

A summary of the scenarios considered, and the parameters specified for the simulations in IDA ICE can be seen in Table 2.

2.3. *Ventilation rates and room CO_2 concentration*

The air flow rate measurements were carried out on the experimental setup, using a rotating vane anemometer (Testo 417) with an air-cone (i.e. funnel) attachment. Since the fan speed was controlled by a 10-step potentiometer, the measurements were conducted at the highest (10/10), medium (6/10) and lowest (1/10) fan speeds. These empirically determined values for the air flow rate were then implemented as ventilation boundary conditions in the IDA ICE dynamic simulation tool for scenarios 2 and 3 (see Section 2.2 for information on the dynamic

Table 3
Limit CO_2 concentration according to EN 16798–1:2019.

IEQ-Categories	default design		Level ofexpectation
	above outdoor CO_2 conc. [ppm][1]	Total CO_2 conc. [ppm][2]	
1	550	970	High[3]
2	800	1220	Medium[4]
3	1350	1770	Moderate
4	1350	1770	Low

[1] CO_2 values correspond to an air flow rate of 10, 7, 4 L/s (per person) for categories 1, 2, 3 respectively with a CO_2 emission of 20 L /h (per person) [42].
[2] Current outdoor CO_2 concentration of approx. 420 ppm [75].
[3] for occupants with special needs (children, elderly) [42].
[4] typically applied level of expectation (Pre-COVID-19) [42].

simulation and Section 3.1 for the measured air flow rates and control mechanisms). To determine how the measured airflow rates affected the IAQ and to find an optimal control strategy for ventilation rates at different occupancy levels, an approach described in the European standard EN 16798–1: 2019 "Energy performance of buildings – Ventilation for buildings" was used [42]. In method 2 of this standard, the design ventilation air flow rates are determined in order to meet defined categories of indoor environmental quality (IEQ), as listed in Table 3. This standard pre-dates the COVID-19 pandemic however, and with knowledge of the airborne transmissivity of SARS-CoV-2 higher ventilation rates (corresponding to CO_2 concentrations at or below category IEQ_1) have since been recommended, as a prophylaxis measure [47,79–81].

The ventilation rate Q_h [L/s] required to dilute a particular air pollutant (i.e. CO_2) is assessed based on a mass balance equation (Eq. 1). The indoor CO_2 concentration was derived from the modelled air flow rates, under the assumption of a standard adult CO_2 emission rate (of 20 L/(h per person) for sedentary activities [42,82]).

$$Q_h = \frac{G_h}{C_{h,i} - C_{h,o}} * \frac{1}{\varepsilon_v} \quad (1)$$

where,

Q_h is the ventilation rate required for dilution of the pollutant (CO_2) [L/s],

G_h is the generation rate of the substance, assuming a standard CO_2 emission rate of 20 L/(h per person) [42,82],

$C_{h,i}$ is the guideline value for the CO_2 concentration [ppm],

$C_{h,o}$ is the CO_2 concentration in the supply air [ppm],

ε_v is the ventilation effectiveness (note: augmentation of the ventilation effectiveness due to displacement ventilation was not included in the BPS and infection risk models, see 'Limitations' in Section 4).

2.4. Infection risk assessment

The risk of infection through aerosol transmission due to the original circulating Omicron variant of the SARS-CoV-2 virus was estimated with an analytical method developed by researchers from the MPIC, Germany, and the Cyprus Institute, Cyprus [57]. The purpose of this infection risk calculation was not to accurately predict the probability of an individual infection occurring at a given point in time (since this would require detailed knowledge of the corresponding time varying community prevalence etc). Rather the purpose of this analysis was to provide an estimate of the relative infection risk, in order to compare the prophylaxis benefits of the different ventilation strategies studied. It was therefore assumed that one person present in the room was already infected with COVID-19 in each case. The risk of infection was analysed for 20 occupants in the room, as this number resulted in a CO_2 concentration compliant with category IEQ_1 of EN 16798–1 in scenario 2 and 3 (see Section 3.1). In this way, the effects of a category IEQ_1 requirement on the incidence of infection was analysed. To evaluate the effect of wearing masks, two cases were compared, one where the occupants did not wear masks and another where they wore FFP2 masks. It should be noted that the analytical infection risk model assumes that the room air and thus the concentration of potentially infectious particles in the room is well mixed (thus ignoring the potential benefits of stratification, see 'Limitations' in Section 4). Furthermore, direct infection by short-range (i.e. large droplet) transmission is not included in the model. Thus, only the indirect (i.e. long range) airborne transmission via aerosols is assessed using this method [57]. The analytical method according to Lelieveld et al. [57,83], along with the associated formulas and parameters which were adopted can be found in Appendix A3.

It has been demonstrated experimentally (using aerosol measurements) that the MPIC-MEV system directly captures between 30% (in the least favourable case) and up to 60% (in the most favourable case) of the potentially infectious aerosols [56]. In this way, the airborne particles are prevented from spreading throughout the room and the risk of infection can be further reduced. Thus for the calculation of the infection risk in scenario 2, a hood efficiency of 0.3 (see appendix A3) was conservatively assumed, which means that in the analytical model 30% of the potentially infectious aerosols are assumed to be extracted at source by the MPIC-MEV system [57]. The calculations were performed for seminar room conditions using volumetric flow rates and boundary conditions determined dynamically by the IDA ICE model.

3. Results & analysis

3.1. Measured ventilation rates

The ventilation air flow of the MPIC-MEV system, as measured with a rotating vane anemometer showed a flow rate of 215 L/s (774 m^3/h) for the highest fan speed (10/10), 140 L/s (505 m^3/h) for the medium speed (6/10), and 90 L/s (322 m^3/h) for the lowest speed (1/10). By substituting these values into (Eq. 1) (Section 2.3) according to Method 2 of EN 16798–1 [42], the IAQ can be assessed as a function of the CO_2 concentration. Fig. 2 shows the indoor CO_2 concentration curves as a function of the ventilation rate for three different levels of occupancy (n = 10, 20, 30). The airflow rates for the middle (blue arrow) and maximum fan speeds can be seen in Fig. 2 (orange arrows). At the maximum fan speed an airflow rate of 215 L/s, compliant with EN 16798–1:2019 category IEQ_1 was met for 10 (21.5 L/s (per person)) and 20 occupants (10.8 L/s (per person)) in the room. For 30 occupants (7.2 L/s (per person)), only category IEQ_2 could be ensured. To compensate for unnecessary ventilation heat losses (due to over-ventilation) at low occupancy (n = 10), it was decided to operate the fan at a medium speed with 140 L/s for 10 people (i.e. 14.0 L/s (per person)) in the room. In this way, the air exchange rate was reduced without compromising category IEQ_1 for air quality. Identical operating conditions were implemented in the IDA ICE simulation for scenarios 2 (MPIC-MEV) and 3 (AHU-HRV) to ensure like-for-like comparisons between the hybrid and mechanical systems.

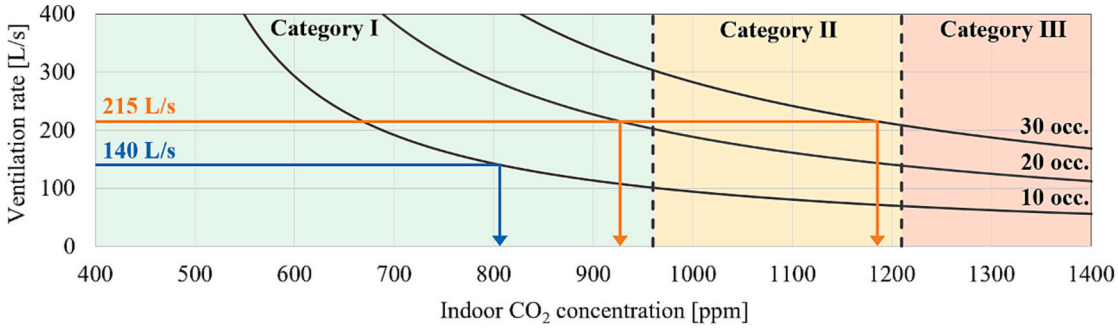

Fig. 2. Indoor CO_2 concentration [ppm] curves in relation to ventilation rate [L/s] under three occupancy levels (10, 20 and 30 persons) and EN 16798–1:2019 threshold limit CO_2 concentration [ppm].

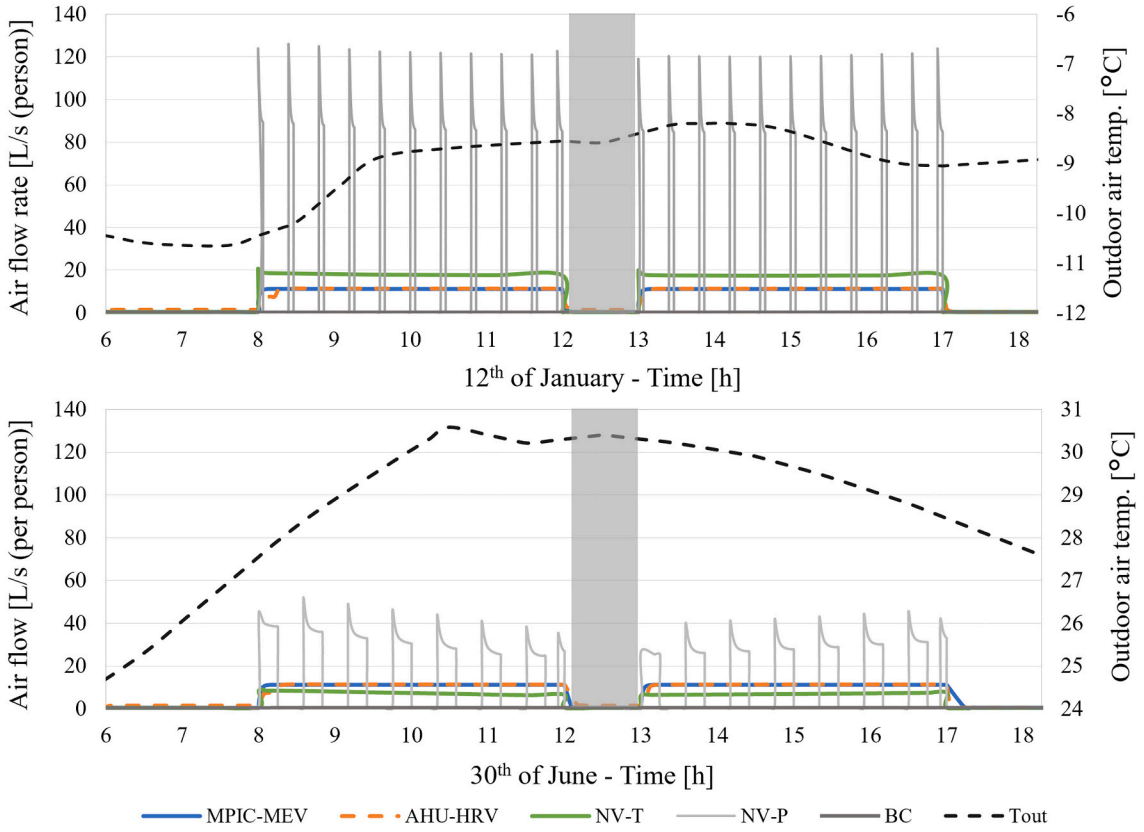

Fig. 3. Temporal profile of room air flow rates on two design days: 12th January - coldest day (top) and 30th June - warmest day (bottom). Note: (i) the blue line (MPIC-MEV) is directly beneath the dashed orange line (AHU-HRV) (ii) results for average days in heating and cooling season can be found in Appendix A4. Grey bars indicate the lunch break period (12:00–13:00 h) where the ventilation systems are turned off and the room is empty. (For interpretation of the references to colour in this figure legend, the reader is referred to the web version of this article.)

3.2. Building simulation results

3.2.1. Ventilation rates

The air flow rates for the different ventilation strategies were calculated using the IDA ICE software based on the site specific weather file (see Section 2.2). Significant variability in the natural ventilation flow rates, can be seen corresponding to natural variations in the pressure differential at the window opening. Fig. 3 shows the temporal evolution of the air flow rates over the course of two selected days, to illustrate the differences between the coldest (12th January) and warmest (30th June) days of the year.

It was determined that in the hybrid and mechanically ventilated scenarios 2 (MPIC-MEV) and 3 (AHU-HRV), the air flow remained almost constant throughout the year (as might be expected using mechanical driving forces). In contrast, in the naturally ventilated scenarios 4 (NV-T) and 5 (NV-P), the air exchange rate was highest during periods with cold temperatures and decreased during periods with warmer temperatures. The reason for this is that the air flow in naturally ventilated rooms is predominantly driven by wind and thermal buoyancy and is proportional to the square root of the total pressure difference [84], [85, p. 16.13]. Since wind and temperature differences tend to be greater in winter, the natural driving forces that move the air are

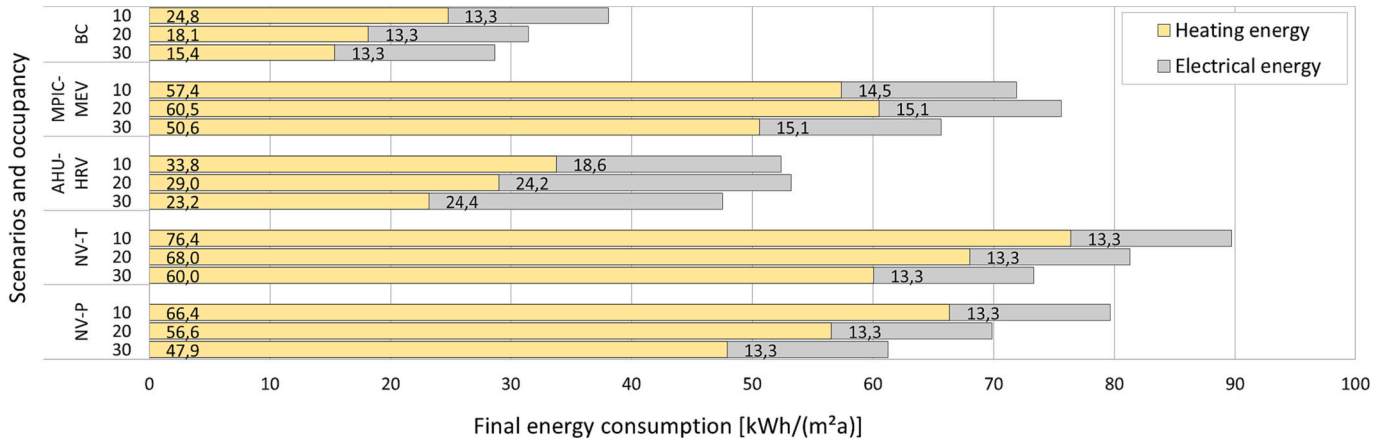

Fig. 4. Final energy (heating and electrical) consumption [kWh/m^{2}a] for the five scenarios with three different levels of occupancy (n = 10, 20, 30).
[†]Note: Results for primary energy consumption can be found in Appendix A5.

stronger at these times [86]. For scenario 4 (with fixed window openings) this resulted in over-ventilation during winter and under-ventilation during summer conditions. Over-ventilation in winter was also the case to a lesser extend for scenario 5 (with purge ventilation), with CO_2 concentrations reaching values below 600 ppm during some of the purge periods (see Section 3.2.4).

3.2.2. Energy performance

The annual final (heating and electrical) energy consumption was calculated for all 5 scenarios based on three different occupancy densities (10, 20, and 30 occupants). Fig. 4 shows the results of the simulated final energy consumption for each scenario. Final energy is an important metric in the context of educational buildings since it directly reflects the metered energy consumption which the end-user pays for and forms part of the operational energy rating used in Energy Performance Certificates (EPC) and Display Energy Certificate (DEC), as mandated under national implementation of the recast EPBD [87].

Scenario 1 (BC) showed the lowest final energy consumption of 32.7 kWh/(m^2a) – averaged over all three occupancy densities – since in this case the windows were never opened during lessons and thus no energy was lost through purposeful ventilation. In scenario 2 (MPIC-MEV), a final energy amount of 71.0 kWh/(m^2a) was consumed on average (119% more than the base case 1). Scenario 3 (AHU-HRV) in comparison reduced this amount to 51.1 kWh/(m^2a) (which was 58% more than the BC and 28% less than scenario 2). Despite saving 27.5 kWh/(m^2a) of heating energy by using heat recovery (under identical boundary conditions) cf. MPIC-MEV, these savings were partially offset by the increased fan power requirement of scenario 3, which resulted in an average of 7.5 kWh/(m^2a) higher electricity consumption than in scenario 2, producing a net final energy saving of 19.9 kWh/(m^2a) corresponding to a primary energy saving of 22.8 kWh/(m^2a) (see Appendix A5). The hybrid (MPIC-MEV) and mechanical (AHU-HRV) ventilation strategies showed their highest final energy consumption with 20 occupants in the room. This was due to the higher ratio of air exchange to occupants needed to achieve the EN 16798–1 Cat. 1 target cf. 10 or 30 occupants (see Section 3.1). However, as expected, a steady reduction in the auxiliary heating energy demand was recorded as the number of students in the room increased. This can be explained by the higher internal heat gains from the occupant's metabolic heat production, which corresponded to 126 W (sensible and latent heat) per person at 1.2 met [74]. Scenario 4 (NV-T) showed the highest average final energy consumption with 81.5 kWh/(m^2a), approximately 150% more than the base case. It was also found that scenario 4 consumed on average 15% more heating energy than scenario 2. The difference in heating energy consumption between these scenarios resulted from the higher air exchange rate occurring in scenario 4, as a function of the internal – external temperature difference during the cold winter period. Dynamically varying the number of tilted windows in the winter period (in accordance with the CO_2 concentration) may have saved energy whilst achieving the targeted ventilation rates, however this was not tested. In comparison, some energy savings were obtained in scenario 5 (NV-P) due to the more targeted short-term opening of the windows. An average energy consumption of 70.3 kWh/(m^2a) was determined for scenario 5, which was 115% more than in scenario 1 and 14% less than with scenario 4 and therefore comparable to scenario 2. Despite similar final energy consumption it should be noted that in scenario 2 there was a continuous air exchange (and therein contaminant removal) whilst in scenario 5 there was only a periodic air exchange every 20 min. It can be seen the targeted regulation of the air flow with fans at colder outdoor temperatures leads to a net increase in energy efficiency (compared to the NV scenarios) – despite the power consumption required by the fans.

To gain a better insight into the energy consumption of the different ventilation systems, the heating load curves were mapped with the corresponding outdoor temperatures over the course of the coldest day. The results are shown in Fig. 5 for an occupancy of 20 people.

The maximum heat load was reached on the 12th of January at a mean daily outdoor temperature of −9 °C. Even at this temperature, heat losses due to infiltration and transmission, during the occupied period, in the base case scenario were fully compensated by internal heat gains (i.e. when no ventilation measures were taken). Scenario 2 displayed a mean heating load of approximately 95 W/m^2 during the occupied period. With the same air exchange rate, whilst the heating load in scenario 3 was greatly reduced (by heat recovery) to an average load of 16 W/m^2. Scenario 4 showed a mean heating load of 107 W/m^2. Due to the very high air exchange rates during purge ventilation, scenario 5 showed a fluctuating heating load, with a mean heating load of 70 W/m^2 and peak loads reaching 140 W/m^2 over the 8 h period.

3.2.3. Thermal comfort

In this section, thermal comfort conditions are assessed in line with international standards [42,74] on the basis of the operative temperature, which can be calculated with sufficient approximation as the average of the air temperature and mean radiant temperature (when internal air speeds are below 0.1 m/s) [88]. The operative room temperature was simulated dynamically with IDA ICE. Fig. 6 shows the temporal profile of the operative temperature corresponding to the respective ventilation strategies over the course of the coldest day (12th of January). The results are presented for an occupancy of 20 people (since for this occupancy the ratio of the supply air exchange rate to the internal heat gains was the least favourable in cold weather).

At a constant heating setpoint air temperature of 20 °C (using a 2 °C P-band for proportional temperature control) in the simulation, it was

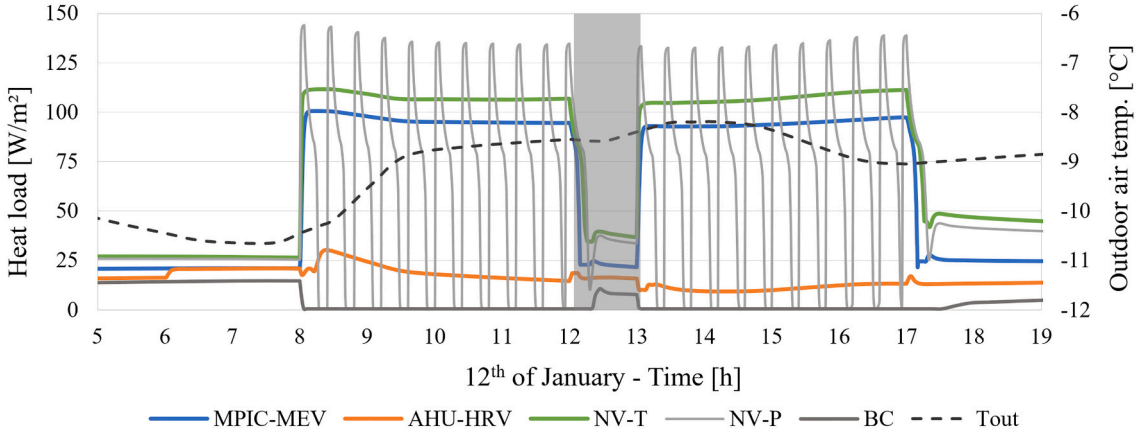

Fig. 5. Heating load density [W/m^2] for 20 occupants, on the coldest day in winter. Note: Results for average days during the heating and cooling seasons can be found in Appendix A4. Grey bars indicate the lunch break period (12:00–13:00 h) where the ventilation systems are turned off and the room is empty.

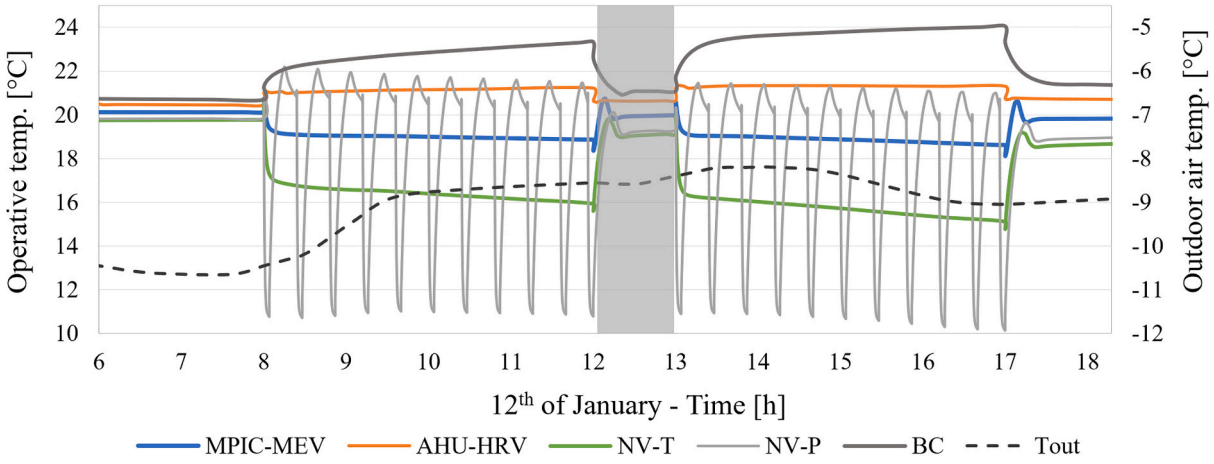

Fig. 6. Operative temperature [°C] for 20 occupants on the coldest day in winter.
Note: Results for average days in heating and cooling season can be found in Appendix A4. Grey bars indicate the lunch break period (12:00–13:00 h) where the ventilation systems are turned off and the room is empty.

found that the average room temperature of the model was strongly dependent on the outdoor temperature profile – especially in the naturally ventilated scenarios. On the 12th of January at an average outdoor temperature of −9 °C, operative temperatures around 23 °C were obtained for the base case scenario during occupation (as there were no purposeful ventilation heat losses). During the occupied period scenario 2 showed constant temperatures of approximately 19 °C throughout, thereby maintaining acceptable thermal conditions. This was due to the use of demand-oriented ventilation rates combined with the high internal heat gains from 20 occupants. Scenario 3 displayed a constant operative temperature of 21 °C during the coldest day of the year, thus ensuring a comfortable thermal state. Ventilation with tilted windows (scenario 4) produced operative temperature values in the range of 15 °C to 17 °C. In contrast, purge ventilation (scenario 5) with intermittently open windows caused temperatures to vary significantly (between 10 °C and 21 °C). Both scenarios with natural ventilation consequently

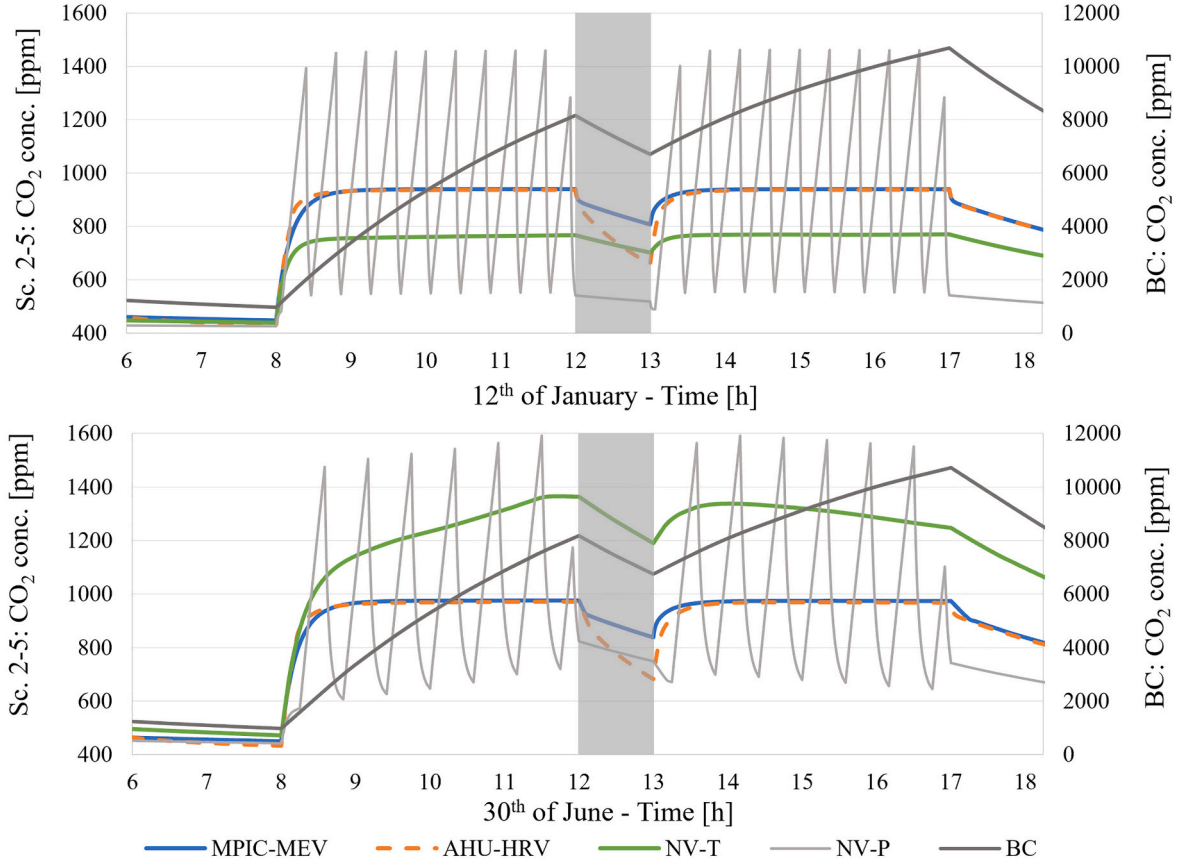

Fig. 7. Indoor CO_2 concentration [ppm] for 20 occupants on two example design days: 12th of January - coldest day (top) and 30th of June - warmest day (bottom).
Note: (i) the blue line (MPIC-MEV) is partially concealed by the orange dashed- line (AHU-HRV). (ii) results for an average day during the heating season can be found in Appendix A4. Grey bars indicate the lunch break period (12:00–13:00 h) where the ventilation systems are turned off and the room is empty.

indicated a significant loss of thermal comfort during the coldest time of the winter period.

3.2.4. Indoor air quality

The indoor CO_2 concentration was simulated dynamically over the whole year, based on the assumption of constant CO_2 emission rates (see Section 2.3). Two design days (12th January and 30th of June) were selected to illustrate the effect of cold (−9 °C, daily average external air temperature) and warm (27 °C, daily average external air temperature) boundary conditions (respectively) on the internal room environment. The purpose of this analysis was to understand the influence of more extreme external conditions on the resultant IAQ. Fig. 7 shows the results of this analysis.

Note that the indoor CO_2 concentration of the base case (black line, Fig. 9) is an order of magnitude higher than the other scenarios and was therefore mapped onto the secondary y-axis using a different scaling. This is the reason for the apparently lower slope of the base case CO_2 concentration when compared to the other scenarios. It was determined that in scenario 1, the CO_2 concentration increased to over 10,600 ppm (at the end of the afternoon) for 20 people due to the lack of ventilation, this value far exceeds the ventilation guidelines set out in EN 16798–1 [42]. The elevated CO_2 concentrations observed in scenario 1 result from the assumption that only passive ventilation with an infiltration rate of 0.17 L/s(m^2) (see Appendix A2) is present during an 8-h occupancy period. While other studies have found CO_2 concentrations above 4500 ppm [52] and as high as 6000 ppm [89] in classrooms with active ventilation, it is important to note that the result of this base case scenario serves as a theoretical worst case comparison within the defined boundary conditions. It should also be noted that the CO_2 values shown for scenario 2 do not take into account hood capture effects (i.e. direct extraction of CO_2) nor displacement effects, which would result in an improvement of the ventilation effectiveness due to the supply of fresh air near the floor, at low air velocities, combined with the extraction of warmer stale air near the ceiling [56], (see 'Limitations' in Section 4). In scenarios 2 and 3 the airflow was mechanically driven so that constant air exchange rates were achieved throughout the year. As a result, scenarios 2 and 3 showed very similar CO_2 concentration trends; with 20 people present in the room, steady values of about 950 ppm were reached, thus complying with the category IEQ_1 limits of EN 16798–1:2019 [42]. Scenario 2, in contrast to scenario 3, achieved a greater decrease in the CO_2 concentration during the 1-h lunchbreak period. This is not an inherent benefit of using an AHU but arose through the use of a set-back mode (0.5 air exchanges per hour), which was implemented in the conventional AHU (scenario 3) scheduling, in accordance with operational guidance in EN 16798–1 [42].

Investigation of the IAQ also revealed that the CO_2 concentration in the naturally ventilated scenarios (4 and 5) was highly dependent on the outdoor air temperature. Therefore, IAQ was best in winter when the pressure difference between inside and outside (and hence the air exchange rate) was highest. The opposite was true for warm summer days when the wind was weaker and the temperature differences between inside and outside were lower. On the 12th of January indoor CO_2 concentrations of approximately 770 ppm were reached in scenario 4. In contrast using intermittent purge ventilation (scenario 5) the CO_2 concentrations in the phases in which the windows were closed varied from 580 to 1450 ppm. On the warmest day of the year (30th of June), with 20 occupants in the room at an average outdoor temperature of 27 °C, the indoor CO_2 concentrations in scenario 4 ranged from 1000 to 1350 ppm during the lecture periods. In scenario 5 (using extended purge cycles) the values varied between 600 and 1600 ppm. Consequently,

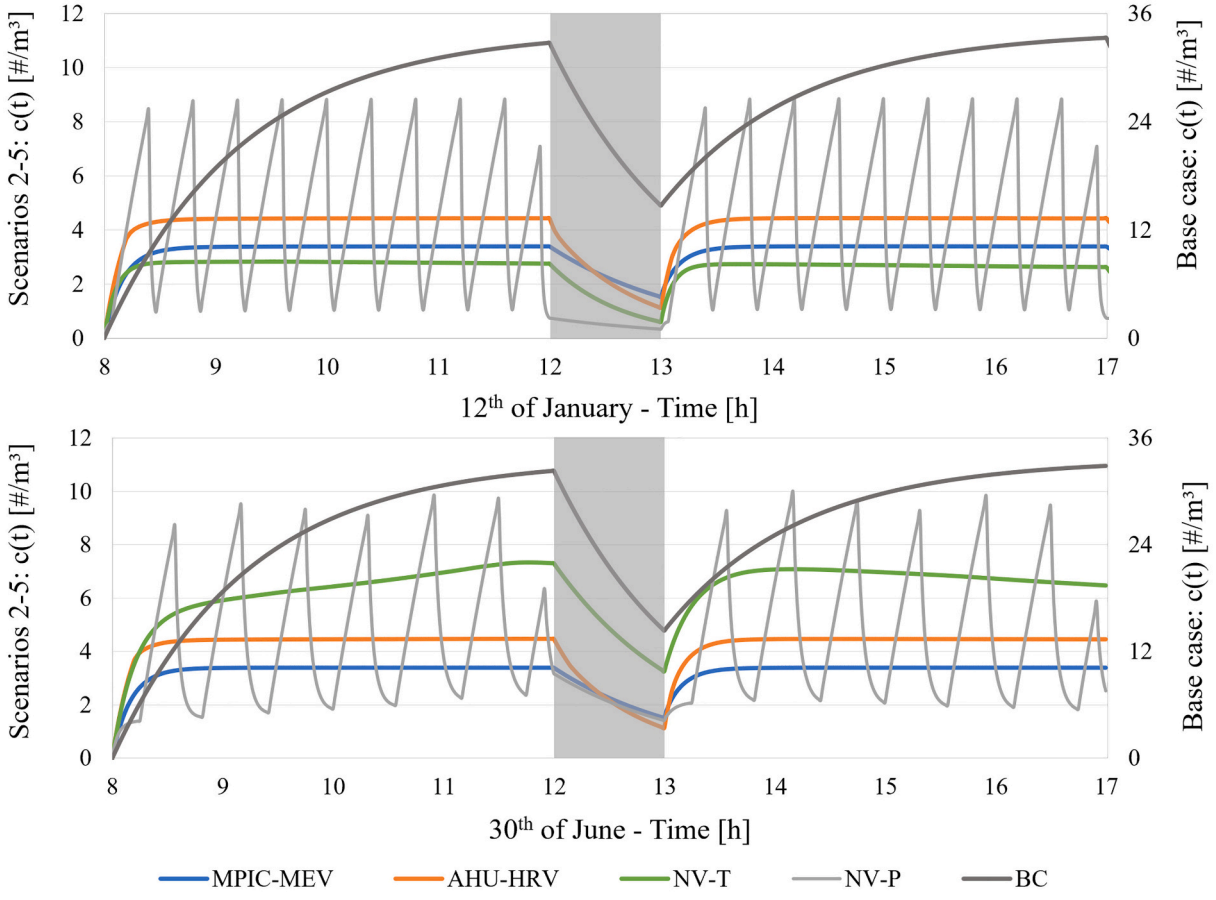

Fig. 8. Virus concentration [#/m^3] as a function of time for 20 unmasked occupants on two example design days: 12th of January - coldest day (top) and 30th of June - warmest day (bottom). Grey bars indicate the lunch break period (12:00–13:00 h) where the ventilation systems are turned off and the room is empty.

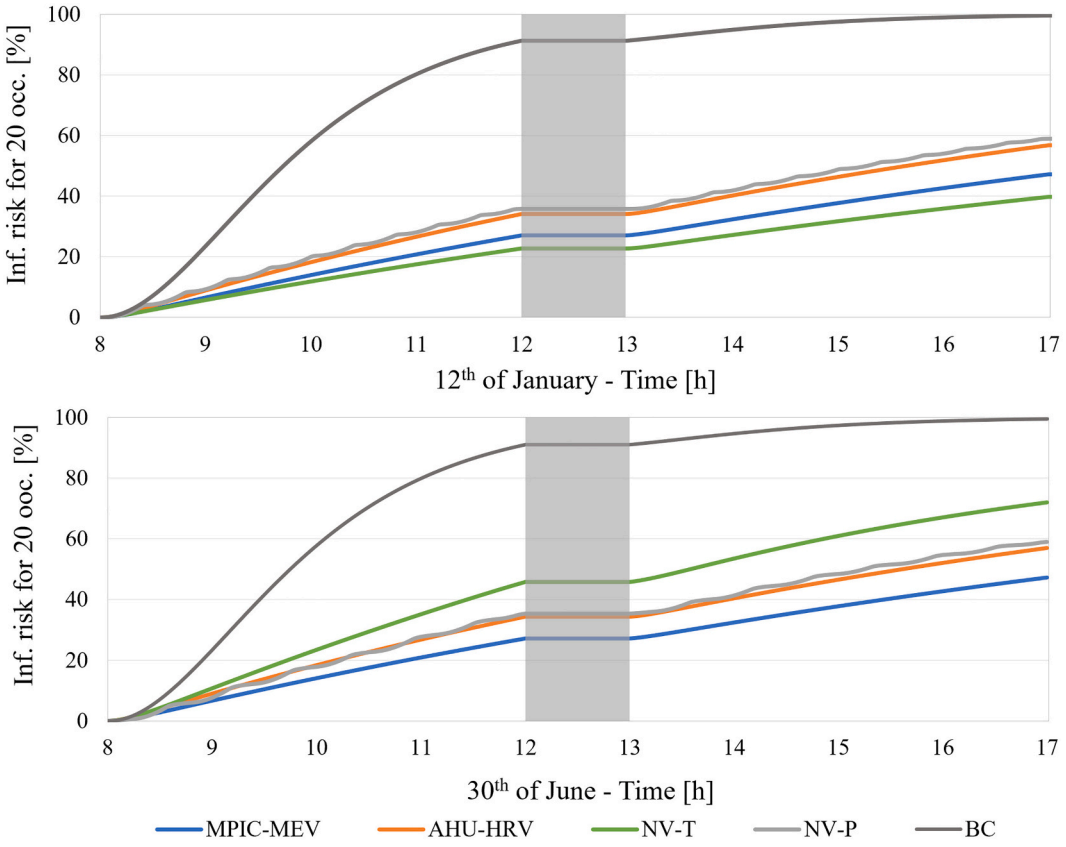

Fig. 9. Probability of at least one infection as a function of time for 20 unmasked occupants on two example design days: 12th of January - coldest day (top) and 30th of June - warmest day (bottom). Grey bars indicate the lunch break period (12:00–13:00 h) where the ventilation systems are turned off and the room is empty.

Table 4
Infection risk probability [%] for any one individual in a group of 20 people with and without universal FFP2 masking after 8 h of exposure on the 12th of January - coldest day (left) and the 30th of June - warmest day (right).

Scenarios	Risk for 12th of January [%]		Risk for 30th of June [%]	
	Without masks	With masks	Without masks	With masks
1. BC	100	27	100	27
2. MPIC-MEV	47	4	47	4
3. AHU-HRV	57	5	57	5
4. NV-T	42	3	72	7
5. NV-P	59	5	59	5

scenario 5 would require a prolonged ventilation duration (i.e. >15 min every 20 min) or fully open windows throughout the occupied period to maintain adequate IAQ during the warmest days of the summer months. Consequently, with full occupancy (n=30) under such conditions it might not be possible to maintain the CO_2 value below a 1000 ppm threshold.

3.3. Infection risk assessment

The risk of infection by the original Omicron variant of the SARS-CoV-2 virus, under the different ventilation scenarios, were similarly analysed for 20 occupants on the two selected design days (i.e. 12th January and 30th June). Fig. 8 shows the build-up of virus-containing respiratory aerosol concentration in the room air $c(t)$ and Fig. 9 the resulting group infection risk as a function of time. The latter is the combined probability that at least one susceptible person from any of the group members (of $n = 20$ people) will become infected. In addition, Table 4 displays the group risk after an 8-h exposure period, respectively for the cases with and without universal FFP2 masking (i.e. irrespective of their COVID-19 status with an assumed mask filter efficiency of 70% for inhalation and 80% for exhalation [83]).

Note that, due to the higher viral concentration, the base case (scenario 1) is depicted on the secondary axis with a different scaling (Fig. 8). Therefore, the slope appears disproportionally low compared to the other scenarios. It can be seen that at a constant air exchange rate, a state of equilibrium was reached in the virus particle concentration present in the room (Fig. 8) analogous to what was determined in the simulation results of the indoor CO_2 concentration (Fig. 7). Conversely, as might be expected, varying air exchange rates were found to result in fluctuating virus particle concentrations.

The results showed the highest risk of infection for scenario 1, as there is no active ventilation in the base case. Under this scenario, based on an occupancy of 20 persons, there was a probability of 100% that at least one person in the room would become infected with SARS-CoV-2 during the 8-h exposure period. If all people present in the room were to wear an FFP2 masks, this value could be reduced to 27%. Scenario 2 resulted in a risk of 47% without masking and 4% with masking that one out of the 20 people present in the room would become infected after a duration of 8 h for both the best-case (cold outdoor temperatures) and worst-case (warm outdoor temperatures). Despite the same air exchange rates as for scenario 2, scenario 3 displayed a slightly higher risk of one amongst the 20 occupants becoming infected, with 57% without masking and 5% with masking. This difference between scenarios 2 and 3 can be attributed to the reduced room aerosol emission intensity achieved by the distributed (i.e. localised) extraction of potentially infectious aerosols using the MPIC-MEV system extract hoods (further information on the infection risk model and the and the selected parameters can be found in Appendix A4).

In contrast the infection risk under the naturally ventilated scenarios showed a stronger dependence on the outdoor air temperatures. Due to

the relatively high air exchange rates with tilted windows, on the 12th of January, scenario 4 resulted in a combined risk of 42% without masks and 3% with masks. In contrast, with warmer external air temperatures in summer, higher values were found with tilted windows due to the lower air exchange rate. On the 30th of June an infection transmission risk of 72% without masking and 7% with masking for an individual in a group of 20 occupants was found. Scenario 5 showed a higher infection risk under cold outdoor conditions cf. scenarios 2–4 (see Table 4). This was because of the 20-min phases (between purges) in which the room was not ventilated at all. During these phases, the concentration of virus-containing particles sharply increased (in parallel with the indoor CO_2 concentration) to relatively high values (~10 particles per m^3 of room air, see Fig. 8). Intensive short-term purge ventilation strongly reduced this concentration afterwards so that on average similar infection probabilities to scenario 3 were observed. Thus, after an 8-h residence time on January 12th an infection risk probability of 59% without masks and 5% with masks was seen. Despite lower natural driving forces during the summer periods, scenario 5 showed a similar infection risk on the 30th of June as on the coldest winter day, which is due to the extended summer purge duration time (of 15 min) cf. the 4 min duration applied during the winter period. This finding highlights the importance of adjusting purge duration intervals in accordance with outside air temperatures.

4. Discussion

This study made use of building performance simulation combined with analytical infection risk modelling to understand the performance characteristics of different retrofit ventilation strategies designed to mitigate long-range airborne transmission from SARS-CoV-2 in an educational setting. Dynamic thermal simulations were carried out for five different ventilation scenarios to determine the energy performance, IAQ and the prevailing operative temperature conditions in a university seminar room. The airflow rates provided by the hybrid ventilation system constructed in the experimental seminar room were empirically measured and then implemented in the building simulation model. In addition, the SARS-CoV-2 infection risk was analytically assessed, and the results were evaluated in relation to the different ventilation strategies considered. Table 5 provides an overview of all ventilation measures in relation to the different Key Performance Indicators (KPI) assessed in this study.

4.1. Energy performance

In this heating dominated context (Graz, Austria), it was shown that the different ventilation strategies strongly influence the final energy performance of the seminar room. Controlling the air exchange rate, using either hybrid or purely mechanical means, to maintain an appropriate IAQ target can lead to increased energy efficiency (as seen in scenarios 2 and 3). Due to the high air exchange rates in the winter months, long-term ventilation with permanently tilted windows (scenario 4) proved to be inefficient, supporting recommendations for improved control of tilted windows (either manually or via the use of window actuators) at the coldest times of the year [78].

However, it should be noted that final energy is only one metric, and whilst it reflects the economic cost of the energy consumed it does not necessarily reflect the full energetic or climatic impacts of a given system. For this reason consideration of the Primary Energy consumed (see Appendix A5) as well as the embodied energy (or global warming potential) and resources needed to manufacture, maintain, recycle and eventually dispose of an air handling unit are important considerations. For these reasons further energetic, carbon and global warming potential (GWP) analysis (beyond the scope of this study) is warranted.

4.2. Thermal comfort

It was shown that comfortable operative temperatures are met only with the targeted control of ventilation. Despite constant fan driven ventilation (during the occupied hours) a reasonable indoor climate can be maintained (in Graz, Austria), even during the coldest periods of winter, with hybrid (scenario 2) and mechanical (scenario 3) ventilation. Thus, for scenario 2, at the lowest outdoor temperatures, the operative indoor temperatures do not drop below the minimum operative temperature of category IEQ_3 (19 °C) for indoor environmental quality according to EN 16798–1:2019 [42]. In contrast neither natural ventilation scenario manages to achieve the conditions required to maintain minimum temperatures to comply with category IEQ_4 (18 °C) of EN 16798–1:2019 [42] on cold days when the air exchange rate is highest. This indicates that the use of natural ventilation, without continuous adjustment or automated mechanisms, to control the fresh air supply rate, is likely to compromise thermal comfort at these times.

4.3. Indoor air quality

The results of this study show that acceptable IAQ (i.e. not exceeding the target threshold value of 1000 ppm proposed in most international guidelines [45,78]) and indoor environmental quality of category IEQ_1 (established by EN-16798-1:2019 [42]) cannot be achieved by intermittent purge ventilation (scenario 5). Moreover whilst tilted windows (scenario 4) can easily meet the IAQ target in winter, this becomes more challenging in summer and is likely to require additional turned windows to maintain the air quality. In contrast the use of hybrid (scenario 2) or mechanical (scenario 3) ventilation guarantees that the IAQ targets are consistently met year-round (assuming the fans are correctly sized).

It should be noted that the simulation used in this work assumes that windows are correctly opened by occupants according to the established ventilation strategies. However, reality has shown that window ventilation is frequently inadequately operated at colder temperatures in favour of thermal comfort [52,90]. Moreover, a study by Helleis et al. [56], which analysed different ventilation strategies with regard to IAQ

Table 5
Overview of different ventilation measures.

KPI's [a]	1. BC	2. MPIC-MEV	3. AHU-HRV	4. NV-T	5. NV-P
Final energy cons. [kWh/(m^2a)]	33	71	51	82	70
Indoor operative temp. on 12.01 [°C]	23	19	21	15–17	10–21
Indoor air quality peak winter day [ppm] [c]	10600	950	950	770	1450
Indoor air quality peak summer day [ppm] [d]	10600	950	950	1350	1600
Inf. risk for group peak winter day [%] [b,c]	100	47	57	42	59
Inf. risk for group peak summer day [%] [b,d]	100	47	57	72	59

[a] All results shown have been determined for n = 20 occupants.
[b] Probability that at least one susceptible person from the group of $n = 20$ will become infected (assuming all are unmasked).
[c] Peak winter day refers to 12th January (using the EPW TRY climate file for Graz, Austria).
[d] Peak summer day refers to 30th June (using the EPW TRY climate file for Graz, Austria).

and infection prevention in classroom settings, found similar values for the indoor CO_2 concentration for both tilted windows and purge ventilation strategies. However, Helleis et al. have demonstrated considerably lower values (under optimal conditions <600 ppm) for the MPIC mechanical extract ventilation system (scenario 2). This is attributed to the increased ventilation effectiveness associated with incorporation of the displacement ventilation effect, whereas a well-mixed air model was used, as a conservative assumption, in this work.

4.4. Infection risk

It is shown that the CO_2 concentration and the infectious virus particle load in the room are closely dependent on the air exchange rate. Therefore, the hybrid and mechanically ventilated scenarios (2 and 3) show a significantly lower risk of infection due to the continuous fan-driven air supply. In comparison, the naturally ventilated scenarios (4 and 5) exhibit an infection risk profile that is strongly influenced by the outdoor air temperature.

During winter days, when the temperature difference (and the resulting air exchange rate) are the highest, lower infection risks can be seen than in summer. Although scenarios 2, 3 and (in winter) 4 fulfil the IAQ requirements of category IEQ_1 of EN 16798–1, the overall risks in each scenario remain very high. Even with the best performing hybrid ventilation system (MPIC-MEV), assuming that one person in the room is infectious, the probability of at least one other person (over an 8-h period, in a seminar room with 20 unmasked occupants) becoming infected with the original Omicron variant exceeds 45%. This value is reduced by an order of magnitude, to approximately 4%, by the additional wearing of FFP2 masks (based on a mask filter efficiency of 70% for inhalation and 80% for exhalation [83]). In contrast, a cohort study conducted in Italy (involving approximately 205,000 students) demonstrated that the probability of infection decreases by up to 80% when mechanical ventilation systems with an airflow of >10 L/s (per person) are used, compared to natural ventilation (i.e. ventilation through infiltration and manual opening of windows) [54]. The differences between the theoretical estimates here and the empirically determined values of Buonanno et al. can be explained by the protective measures taken and the lower infectiousness of the Delta variant of the SARS-CoV-2 virus (predominant at the time of the study) [54] as well as the oftentimes insufficient natural ventilation found in the comparator schools [53]. Nevertheless, both findings highlight the significant benefit of using multiple prophylaxis measures, in combination, when community transmission rates are high.

4.5. Limitations

It should be noted that the building simulation and infection risk models used in this work exclude the modelling of displacement effects (i.e. temperature driven buoyancy) which are anticipated to further improve the ventilation effectiveness of displacement ventilation (scenario 2) by between 25 and 50% [56]. However this effect needs to be established empirically under transient boundary conditions (along with the temperature dependent hood capture effect), before being reliably incorporated into the models in the form of increased ventilation effectiveness. Moreover, a higher ventilation effectiveness would achieve similar or better indoor air quality at a lower air change rate, thereby reducing the energy costs associated with scenario 2 [91].

Although this study focuses primarily on local impacts in one seminar room, it is also important to consider educational building as a whole, since they typically have lower overall occupancy and ventilation rates per square meter. In this larger context, heat losses through the building envelope may become a predominant factor.

The simulation applied in this work assumes perfect installation, maintenance, performance, etc. of mechanical systems, as well as the timely opening of windows by occupants based on ventilation requirements. Reality has shown that mechanical systems are often poorly designed, commissioned and operated [92] whilst occupant behaviour varies greatly and is difficult to predict, which is why simulated results often differ from reality [52].

Further, it is important to add that the infection risk model used assumes an immunologically naive population (i.e. without acquired viral antibodies or T-cell immunity). As a result, actual infection rates may be lower at times than estimated here, due to the increased seroprevalence of antibodies [93,94].

It should be noted that the assessment of thermal comfort used in this study was based on a single node (centre of room) calculation and that higher resolution thermal comfort assessments would be needed to assess the thermal comfort response at every seated position in the room.

5. Conclusion

In this study, the performance of five different ventilation strategies (natural, mechanical and hybrid) was evaluated in terms of key performance indicators including energy consumption, thermal comfort, CO_2 concentration, and SARS-CoV-2 infection risk.

It was found that a trade-off between acceptable indoor air quality, reduced infection risk, thermal comfort and energy efficiency can be met throughout the year using either hybrid or mechanical ventilation methods which are specifically designed to meet the actual ventilation requirements of the space. In contrast, without some form of automated control, it is almost impossible for natural ventilation strategies alone to fulfil all of these objectives at the same time, due to their high dependence on external conditions and occupant behaviour. Moreover, the SARS-CoV-2 infection risk modelling showed that without masking or additional prophylaxis measures none of the ventilation strategies modelled here can achieve safe operating conditions over an 8-h period, assuming that an infectious person is already present in the room. The results of this study demonstrate the need for a holistic approach to HVAC system design, which considers not only the energy efficiency of buildings, in relation to heating and cooling needs, but also the complex relationships between indoor air quality and associated health factors, including the risk of infection from respiratory viruses and impacts on thermal comfort. Alongside these factors there are a number of further considerations, including air pollution issues, acoustic comfort, whole life costs and climate change impacts, which should be considered by subsequent studies adopting a holistic multi-criteria decision making approach to ventilation design.

CRediT authorship contribution statement

Fatos Pollozhani: Writing – review & editing, Writing – original draft, Methodology, Investigation, Formal analysis, Conceptualization. **Robert S. McLeod:** Writing – review & editing, Writing – original draft, Supervision, Methodology, Investigation, Formal analysis, Conceptualization. **Christian Schwarzbauer:** Writing – review & editing. **Christina J. Hopfe:** Writing – review & editing, Writing – original draft, Supervision, Methodology, Investigation, Formal analysis, Conceptualization.

Declaration of Competing Interest

The authors declare that the research was carried out in the absence of any commercial or financial relationships that could be considered a potential conflict of interest.

Data availability

No empirical datasets were used for the research described in the article.

Acknowledgements

This research was made possible by the support for the CovEd project provided by the Graz University of Technology and its rector Univ. Prof. Dipl.-Ing. Dr.techn. Dr.h.c.mult. Harald Kainz. The authors would like to thank the Max Planck Institute for Chemistry in Mainz, in particular Prof. Dr. Ulrich Pöschl, Dr. Frank Helleis and Dr. Thomas Klimach, for sharing their research findings and results at www.ventilation-mainz.de.

Appendix A. Supplementary data

Supplementary data to this article can be found online at https://doi.org/10.1016/j.apenergy.2023.121961.

References

[1] WHO. All schools in Europe and Central Asia should remain open and be made safer from COVID-19, say WHO and UNICEF. https://www.who.int/europe/news/item/30-08-2021-all-schools-in-europe-and-central-asia-should-remain-open-and-be-made-safer-from-covid-19-say-who-and-unicef; 2021 (accessed Dec. 20, 2022).
[2] Moscoviz L, Evans DK. Learning loss and student dropouts during the COVID-19 pandemic: A review of the evidence two years after schools shut down. Center for Global Development; 2022. Working Paper, 609. Accessed: Jan. 25, 2023. [Online]. Available: https://www.cgdev.org/publication/learning-loss-and-student-dropouts-during-covid-19-pandemic-review-evidence-two-years.
[3] Lessler J, Grabowski MK, Grantz KH, Badillo-Goicoechea E, Metcalf CJE, Lupton-Smith C, et al. Household COVID-19 risk and in-person schooling. Science (1979) Jun. 2021;372(6546):1092–7. https://doi.org/10.1126/science.abh2939.
[4] Park E, Choi SY, Lee S, Kim M, Lee K, Lee S, et al. Widespread Household Transmission of SARS-CoV-2 B.1.1.529 (Omicron) Variant from Children, South Korea, 2022. Yonsei Med J 2023;64(5):344. https://doi.org/10.3349/ymj.2022.0608.
[5] Meuris C, et al. Transmission of SARS-CoV-2 after COVID-19 screening and mitigation measures for primary school children attending school in Liège, Belgium. JAMA Netw Open Oct. 2021;4(10). https://doi.org/10.1001/jamanetworkopen.2021.28757. e2128757.
[6] Pierce CA, Herold KC, Herold BC, Chou J, Randolph A, Kane B, et al. COVID-19 and children. Science (1979) Sep. 2022;377(6611):1144–9. https://doi.org/10.1126/science.ade1675.
[7] Altrichter H, Kepler C Helm Johannes. Austrian schools in the COVID-19 pandemic era. Tertium comparationis 2022;28(3):300–31. https://doi.org/10.25656/01:25329.
[8] Ayouni I, Maatoug J, Dhouib W, Zammit N, Fredj S Ben, Ghammam R, et al. Effective public health measures to mitigate the spread of COVID-19: a systematic review. BMC Public Health Dec. 2021;21(1):1–14. https://doi.org/10.1186/S12889-021-11111-1/TABLES/3.
[9] Talic S, Shah S, Wild H, Gasevic D, Maharaj A, Ademi Z, et al. Effectiveness of public health measures in reducing the incidence of covid-19, SARS-CoV-2 transmission, and covid-19 mortality: systematic review and meta-analysis. BMJ Nov. 2021;375. https://doi.org/10.1136/BMJ-2021-068302.
[10] Wang C, Wang D, Abbas J, Duan K, Mubeen R. Global financial crisis, smart lockdown strategies, and the COVID-19 spillover impacts: a global perspective implications from Southeast Asia. Front Psych Sep. 2021;12:1099. https://doi.org/10.3389/FPSYT.2021.643783/BIBTEX.
[11] Wieland V. Overview of how major economies have responded to the Covid-19 pandemic. Belgium: EPRS: European Parliamentary Research Service; Feb. 2022. Accessed: Feb. 08, 2023. [Online]. Available: https://policycommons.net/artifacts/2264710/overview-of-how-major-economies-have-responded-to-the-covid-19-pandemic/3023744/.
[12] de Soyres F, Santacreu AM, Young H. The Fed - Fiscal policy and excess inflation during Covid-19: a cross-country view. Board of Governors of the Federal Reserve System (U.S.); Jul. 15, 2022. https://www.federalreserve.gov/econres/notes/feds-notes/fiscal-policy-and-excess-inflation-during-covid-19-a-cross-country-view-20220715.html (accessedFeb. 08, 2023).
[13] UNESCO. UNESCO COVID-19 education response: how many students are at risk of not returning to school? Advocacy paper. UNESCO; 2020. Accessed: Jan. 25, 2023. [Online]. Available: https://unesdoc.unesco.org/ark:/48223/pf0000373992.
[14] Bock-Schappelwein J, Famira-Mühlberger U, Kogler M, Weingärtner S. Die COVID-19-Pandemie und Schule. Eine bildungsökonomische Kurzanalyse. Österreichisches Institut für Wirtschaftsforschung; Sep. 2021. Accessed: Dec. 20, 2022. [Online]. Available: https://www.wifo.ac.at/jart/prj3/wifo/resources/person_dokument/person_dokument.jart?publikationsid=67333&mime_type=application/pdf.
[15] UNICEF. Impact of COVID-19 on children living in poverty - Technical note. Accessed: Jan. 25, 2023. [Online]. Available: https://data.unicef.org/resources/impact-of-covid-19-on-children-living-in-poverty/; 2021.
[16] Irwin M, Lazarevic B, Soled D, Adesman A. The COVID-19 pandemic and its potential enduring impact on children. Curr Opin Pediatr Feb. 2022;34(1):107. https://doi.org/10.1097/MOP.0000000000001097.
[17] Lehmann S, Skogen JC, Haug E, Mæland S, Fadnes LT, Sandal GM, et al. Perceived consequences and worries among youth in Norway during the COVID-19 pandemic lockdown. Scand J Public Health Nov. 2021;49(7):755–65. https://doi.org/10.1177/1403494821993714/SUPPL_FILE/SJ-PDF-1-SJP-10.1177_1403494821993714.PDF.
[18] Segre G, Campi R, Scarpellini F, Clavenna A, Zanetti M, Cartabia M, et al. Interviewing children: the impact of the COVID-19 quarantine on children's perceived psychological distress and changes in routine. BMC Pediatr Dec. 2021;21(1):1–11. https://doi.org/10.1186/S12887-021-02704-1/TABLES/2.
[19] Viner R, Russell S, Saulle R, Croker H, Stansfield C, Packer J, et al. School closures during social lockdown and mental health, health behaviors, and well-being among children and adolescents during the first COVID-19 wave: a systematic review. JAMA Pediatr Apr. 2022;176(4):400–9. https://doi.org/10.1001/JAMAPEDIATRICS.2021.5840.
[20] Passavanti M, Argentieri A, Barbieri DM, Lou B, Wijayaratna K, Foroutan Mirhosseini AS, et al. The psychological impact of COVID-19 and restrictive measures in the world. J Affect Disord Mar. 2021;283:36–51. https://doi.org/10.1016/J.JAD.2021.01.020.
[21] Gurdasani D, Pagel C, McKee M, Michie S, Greenhalgh T, Yates C, et al. Covid-19 in the UK: policy on children and schools. BMJ Aug. 2022;378. https://doi.org/10.1136/BMJ-2022-071234.
[22] Adams R. 'Cultural shift' since pandemic causing attendance crisis in English schools. The Guardian 2023. https://www.theguardian.com/education/2023/jan/13/cultural-shift-since-pandemic-causing-attendance-crisis-in-english-schools (accessed Apr. 18, 2023).
[23] Mehta J. 3 years since the pandemic wrecked attendance, kids still aren't showing up to school. npr 2023. https://www.npr.org/2023/03/02/1160358099/school-attendance-chronic-absenteeism-covid (accessed Apr. 18, 2023).
[24] Villani L, D'Ambrosio F, Ricciardi R, de Waure C, Calabrò GE. Seasonal influenza in children: costs for the health system and society in Europe. Influenza Other Respi Viruses Sep. 2022;16(5):820–31. https://doi.org/10.1111/IRV.12991.
[25] Nazareth J, Pan D, Martin CA, Barr I, Sullivan SG, Stephenson I, et al. Is the UK prepared for seasonal influenza in 2022–23 and beyond? Lancet Infect Dis Sep. 2022;22(9):1280–1. https://doi.org/10.1016/S1473-3099(22)00503-5.
[26] Marani M, Katul GG, Pan WK, Parolari AJ. Intensity and frequency of extreme novel epidemics. Proc Natl Acad Sci U S A Aug. 2021;118(35). https://doi.org/10.1073/PNAS.2105482118/SUPPL_FILE/PNAS.2105482118.SAPP.PDF. e2105482118.
[27] Fisk WJ. The ventilation problem in schools: literature review. Indoor Air Nov. 2017;27(6):1039–51. https://doi.org/10.1111/INA.12403.
[28] Hutter HP, Haluza D, Piegler K, Hohenblum P, Fröhlich M, Scharf S, et al. Semivolatile compounds in schools and their influence on cognitive performance of children. Int J Occup Med Environ Health Jan. 2013;26(4):628–35. https://doi.org/10.2478/S13382-013-0125-Z/METRICS.
[29] Haverinen-Shaughnessy U, Moschandreas DJ, Shaughnessy RJ. Association between substandard classroom ventilation rates and students' academic achievement. Indoor Air Apr. 2011;21(2):121–31. https://doi.org/10.1111/J.1600-0668.2010.00686.X.
[30] Wargocki P, Porras-Salazar JA, Contreras-Espinoza S, Bahnfleth W. The relationships between classroom air quality and children's performance in school. Build Environ Apr. 2020;173:106749. https://doi.org/10.1016/J.BUILDENV.2020.106749.
[31] Morawska L, et al. How can airborne transmission of COVID-19 indoors be minimised? Environ Int Sep. 2020;142. https://doi.org/10.1016/J.ENVINT.2020.105832. 105832.
[32] Li Y, Cheng P, Jia W. Poor ventilation worsens short-range airborne transmission of respiratory infection. Indoor Air Jan. 2022;32(1). https://doi.org/10.1111/ina.12946.
[33] Stabile L, Pacitto A, Mikszewski A, Morawska L, Buonanno G. Ventilation procedures to minimize the airborne transmission of viruses in classrooms. Build Environ Sep. 2021;202. https://doi.org/10.1016/J.BUILDENV.2021.108042.
[34] Di Gilio A, Palmisani J, Pulimeno M, Cerino F, Cacace M, Miani A, et al. CO2 concentration monitoring inside educational buildings as a strategic tool to reduce the risk of Sars-CoV-2 airborne transmission. Environ Res Nov. 2021;202:111560. https://doi.org/10.1016/J.ENVRES.2021.111560.
[35] Scheff PA, Paulius VK, Huang SW, Conroy LM. Indoor air quality in a middle school, part i: use of co2 as a tracer for effective ventilation. Appl Occup Environ Hyg 2000;15(11):824–34. https://doi.org/10.1080/10473220050175706.
[36] Burridge HC, Fan S, Jones RL, Noakes CJ, Linden PF. Predictive and retrospective modelling of airborne infection risk using monitored carbon dioxide31(5); 2022. p. 1363–80. https://doi.org/10.1177/1420326X211043564.
[37] Peng Z, Jimenez JL. Exhaled CO2 as a COVID-19 infection risk proxy for different indoor environments and activities. Environ Sci Technol Lett May 2021;8(5):392–7. https://doi.org/10.1021/acs.estlett.1c00183.
[38] Pollozhani F, Mcleod RS, Klimach T, Pöschl U, Hopfe CJ. Energy performance and infection risk evaluation of retrofitted ventilation systems in times of covid. In: Proceedings of BauSim Conference 2022. Weimar, Germany: IBPSA - International Building Performance Simulation Association; 2022. Accessed: Feb. 01, 2023. [Online]. Available: https://publications.ibpsa.org/conference/?id=bausim2022.
[39] CIBSE. TM64 Operational performance: Indoor air quality. Accessed: Aug. 02, 2023. [Online]. Available: https://www.cibse.org/knowledge-research/knowledge-portal/operational-performance-indoor-air-quality-emissions-sources-and-mitigation-measures-tm64; 2020.
[40] McLeod RS, Mathew M, Salman D, Thomas CLP. An Investigation of Indoor Air Quality in a Recently Refurbished Educational Building. Front Built Environ. Jan. 2022;7:769761. https://doi.org/10.3389/FBUIL.2021.769761/BIBTEX.
[41] Baloch RM, et al. Indoor air pollution, physical and comfort parameters related to schoolchildren's health: Data from the European SINPHONIE study. Science of the

Total Environment Oct. 2020;739. https://doi.org/10.1016/J.SCITOTENV.2020.139870.
[42] CEN. ÖNORM EN 16798–1. Energetische Bewertung von Gebäuden - Teil 1: Eingangsparameter für das Innenraumklima zur Auslegung und Bewertung der Energieeffizienz von Gebäuden bezüglich Raumluftqualität, Temperatur, Licht und Akustik - Module M1–6. Austrian Standards International; Nov. 01, 2019. Accessed: Dec. 20, 2022. [Online]. Available: https://shop.austrian-standards.at/action/de/public/details/664889/OENORM_EN_16798-1_2019_11_01;jsessionid=CEC2A041D6A2EDF0292D59FA47FC3696.
[43] ISO. ISO 17772-1:2017 - Energy performance of buildings — Indoor environmental quality — Part 1: Indoor environmental input parameters for the design and assessment of energy performance of buildings. Switzerland: ISO 2017; 2017. Accessed: Apr. 17, 2023. [Online]. Available: https://www.iso.org/standard/60498.html.
[44] CIBSE. COVID-19: Ventilation (version 5). London: The Chartered Institution of Building Services Engineers; Jul. 16, 2021. https://www.cibse.org/emerging-from-lockdown (accessed Dec. 20, 2022).
[45] REHVA. Rehva covid 19 guidance. https://www.rehva.eu/activities/covid-19-guidance/rehva-covid-19-guidance; Apr. 15, 2021 (accessed Dec. 20, 2022).
[46] Hopfe CJ, Klimach T, McLeod RS, Pöschl U. Leitfaden zum Gebrauch von CO2-Sensoren zur Verbesserung von Luftqualität und Infektionsschutz in Innenräumen. Wien: Future Operations Plattform; 2022. Accessed: Jan. 03, 2023. [Online]. Available: https://futureoperations.at/fileadmin/user_upload/k_future_operations/Leitfaden-CO2-Sensoren_2022-11-02_Final.pdf.
[47] Rowe BR, Canosa A, Meslem A, Rowe F, et al. Build Environ Jul. 2022;219. https://doi.org/10.1016/J.BUILDENV.2022.109132.
[48] Duval D, Palmer JC, Tudge I, Pearce-Smith N, O'connell E, Bennett A, et al. Long distance airborne transmission of SARS-CoV-2: rapid systematic review. BMJ Jun. 2022;377. https://doi.org/10.1136/BMJ-2021-068743.
[49] Setti L, Passarini F, De Gennaro G, Barbieri P, Perrone MG, Borelli M, et al. Int J Environ Res Public Health Apr. 2020;17(8). https://doi.org/10.3390/IJERPH17082932.
[50] Greenhalgh T, Jimenez JL, Prather KA, Tufeki Z, Fisman D, Schooley R. Transmission of SARS-CoV-2: still up in the air – Authors' reply. The Lancet Feb. 2022;399(10324):519–20. https://doi.org/10.1016/S0140-6736(21)02795-1.
[51] McLeod RS, Hopfe CJ, Bodenschatz E, Moriske HJ, Pöschl U, Salthammer T, et al. A multi-layered strategy for COVID-19 infection prophylaxis in schools: A review of the evidence for masks, distancing, and ventilation. Indoor Air Oct. 2022;32(10). https://doi.org/10.1111/INA.13142.
[52] Schwarzbauer C. Forschungsprojekt 'Sicheres Klassenzimmer': Wirkung verschiedener Lüftungsmethoden hinsichtlich Luftqualität und Infektionsschutz im realen Schulunterricht. Dec. 2022. https://doi.org/10.5281/ZENODO.7496827.
[53] EMPA. More infections in poorly ventilated classrooms. https://www.empa.ch/web/s604/covid-and-co2; 2021 (accessed Dec. 21, 2022).
[54] Buonanno G, Ricolfi L, Morawska L, Stabile L, et al. Front Public Health Dec. 2022;10. https://doi.org/10.3389/FPUBH.2022.1087087.
[55] Klimach T, Helleis F, McLeod RS, Hopfe CJ, Pöschl U. The max Planck Institute for Chemistry mechanical extract ventilation (MPIC-MEV) system against aerosol transmission of COVID-19. 2021. https://doi.org/10.5281/zenodo.5802048.
[56] Helleis F, Klimach T, Pöschl U. Wirksamkeit, Energieeffizienz und Nachhaltigkeit verschiedener Lüftungsmethoden hinsichtlich Luftqualität und Infektionsschutz in Innenräumen: Fensterlüften, Abluftventilatoren, Raumlufttechnik und Luftreiniger. Jan. 2023. https://doi.org/10.5281/ZENODO.7586167.
[57] Lelieveld J, Helleis F, Borrmann S, Cheng Y, Drewnick F, Haug G, et al. Model Calculations of Aerosol Transmission and Infection Risk of COVID-19 in Indoor Environments. Int J Environ Res Public Health 2020;17(21). https://doi.org/10.3390/ijerph17218114.
[58] Persily AK. Evaluating Building IAQ and Ventilation with Indoor Carbon Dioxide. In: Transactions-American society of heating refrigerating and air conditioning engineers. 103; 1997. p. 193–204. Accessed: Jan. 04, 2023. [Online]. Available: https://www.aivc.org/resource/evaluating-building-iaq-and-ventilation-indoor-carbon-dioxide.
[59] Turiel I, Rudy J. Occupant-generated CO2 as an indicator of ventilation rate. 1980.
[60] Cui S, Cohen M, Stabat P, Marchio D. CO2 tracer gas concentration decay method for measuring air change rate. Build Environ Jan. 2015;84:162–9. https://doi.org/10.1016/J.BUILDENV.2014.11.007.
[61] Xing H, Hatton A, Awbi HB. A study of the air quality in the breathing zone in a room with displacement ventilation. Build Environ Aug. 2001;36(7):809–20. https://doi.org/10.1016/S0360-1323(01)00006-3.
[62] Linden PF, Bhagat RK. Displacement ventilation: A viable ventilation strategy for makeshift hospitals and public buildings to contain COVID-19 and other airborne diseases. 2020. https://doi.org/10.1098/rsos.200680.
[63] Bhagat RK, Davies Wykes MS, Dalziel SB, Linden PF, et al. J Fluid Mech 2020;903:F1. https://doi.org/10.1017/jfm.2020.720.
[64] EQUA. IDA ICE. https://www.equa.se/de/ida-ice; 2023 (accessed Dec. 20, 2022).
[65] Equa Simulation AB. Validation of IDA indoor climate and energy 4.0 build 4 with respect to ANSI/ASHRAE standard 140–2004. Accessed: Dec. 20, 2022. [Online]. Available: https://www.equa.se/de/ida-ice/validierung-und-zertifikate; 2010.
[66] Moosberger S, Sahlin P, Zweifel G. IDA ICE CIBSE-validation test of IDA indoor climate and energy version 4.0 according to CIBSE TM33, issue 3. Accessed: May 28, 2022. [Online]. Available at: https://www.equa.se/de/ida-ice/validierung-und-zertifikate; Dec. 2007 [Date accessed: 28/05/2022].
[67] Equa Simulation AB. Validation of IDA Indoor Climate and Energy 4.0 with respect to CEN Standards EN 15255–2007 and EN 15265–2007. Accessed: Dec. 20, 2022. [Online]. Available: https://www.equa.se/de/ida-ice/validierung-und-zertifikate; Apr. 2010.
[68] Meteotest AG. Meteonorm software. https://meteonorm.com/; 2023.
[69] Meteotest. Handbook part II: Theory global meteorological database version 8 software and data for engineers, planers and education. Accessed: Dec. 21, 2022. [Online]. Available: https://meteonorm.com/assets/downloads/mn81_theory.pdf; 2021.
[70] Zelenka A, Czeplak G, D'Agostino V, Weine J, Maxwell E, Perez R, et al. Techniques for supplementing solar radiation network data. 1992.
[71] Lu GY, Wong DW. An adaptive inverse-distance weighting spatial interpolation technique. Comput Geosci Sep. 2008;34(9):1044–55. https://doi.org/10.1016/J.CAGEO.2007.07.010.
[72] Gustin M, Oraiopoulos A, McLeod RS, Lomas K. A new empirical model incorporating spatial interpolation of meteorological data for the prediction of overheating risks in UK dwellings. In: 33rd International on Passive and Low Energy Architecture Conference: Design to Thrive: PLEA 2017 - Edinburgh, United Kingdom. Loughborough University; Jul. 2017. p. 3786–93 [Online]. Available: https://hdl.handle.net/2134/25795.
[73] McLeod RS, Hopfe CJ. Hygrothermal implications of low and zero energy standards for building envelope performance in the UK. J Build Perform Simul Sep. 2013;6(5):367–84. https://doi.org/10.1080/19401493.2012.762809.
[74] ISO. ÖNORM EN ISO 7730. Ergonomie der thermischen Umgebung - Analytische Bestimmung und Interpretation der thermischen Behaglichkeit durch Berechnung des PMV- und des PPD-Indexes und Kriterien der lokalen thermischen Behaglichkeit (ISO 7730:2005). Austrian Standards International; May 01, 2006. Accessed: Dec. 20, 2022. [Online]. Available: https://shop.austrian-standards.at/action/de/public/details/215156/OENORM_EN_ISO_7730_2006_05_01;jsessionid=58A69EF60F731BA000390103609EBBE5.
[75] NOAA/ESRL. Trends in atmospheric carbon dioxide. Global Monitoring Laboratory; 2023. https://gml.noaa.gov/ccgg/trends/global.html#global (accessed Dec. 21, 2022).
[76] Systemair GmbH. Topvex FC02 HWH-L-CAV WRG - systemair. https://shop.systemair.com/de-DE/topvex–fc02–hwh–l–cav–wrg/p391659; 2023 (accessed Dec. 20, 2022).
[77] Mourkos K, McLeod RS, Hopfe CJ, Goodier C, Swainson M. Assessing the application and limitations of a standardised overheating risk-assessment methodology in a real-world context. Build Environ Aug. 2020;181:107070. https://doi.org/10.1016/J.BUILDENV.2020.107070.
[78] UBA. Richtig Lüften in Schulen. https://www.umweltbundesamt.de/richtig-lueften-in-schulen#warum-ist-ein-regelmassiger-luftaustausch-in-klassenzimmern-grundsatzlich-wichtig-und-in-der-pandemie-umso-mehr; Dec. 22, 2021 (accessed Dec. 20, 2022).
[79] EMG and SPI-B. EMG-SPI-B: Application of CO2 monitoring as an approach to managing ventilation to mitigate SARS-CoV-2 transmission. Accessed: Dec. 21, 2022. [Online]. Available: https://www.gov.uk/government/publications/emg-and-spi-b-application-of-co2-monitoring-as-an-approach-to-managing-ventilation-to-mitigate-sars-cov-2-transmission-27-may-2021; 2021.
[80] Légifrance. Arrêté du 27 décembre 2022 fixant les conditions de réalisation de la mesure à lecture directe de la concentration en dioxyde de carbone dans l'air intérieur au titre de l'évaluation annuelle des moyens d'aération - Légifrance. https://www.legifrance.gouv.fr/jorf/id/JORFTEXT000046830005; 2022.
[81] FPS Public Health Food Chain Safety and Environment of Belgium. Ventilation | Coronavirus COVID-19. https://www.info-coronavirus.be/en/ventilation/; 2023 (accessed Jan. 17, 2023).
[82] ISO. ÖNORM EN ISO 16000-26. Innenraumluftverunreinigungen - Teil 26: Probenahmestrategie für Kohlendioxid (CO2) (ISO 16000-26:2012). Austrian Standards International; Jun. 15, 2013. Accessed: Dec. 20, 2022. [Online]. Available: https://shop.austrian-standards.at/action/de/public/details/475728/OENORM_EN_ISO_16000-26_2013_06_15;jsessionid=F044A4D6E2C2704DAD63FE83ACFAC7A6.
[83] Max Planck Institute for Chemistry. COVID-19 Risikorechner für Aerosolübertragung Aerosolübertragung von COVID-19 und Ansteckungsgefahr in Innenbereichen. https://www.mpic.de/4747361/risk-calculator; 2022 (accessed Dec. 20, 2022).
[84] Awbi HB. Ventilation of buildings: second edition. 2nd ed. London: Routledge: Spon Press Taylor &Francis Group; 2003. https://doi.org/10.4324/9780203634479.
[85] ASHRAE. 2021 ASHRAE handbook - fundamentals, SI edition. Atlanta, GA: American Society of Heating, Refrigerating and Air-Conditioning Engineers Inc; 2021.
[86] Linden PF. The fluid mechanics of natural ventilation. Annu Rev Fluid Mech 1998;31(1):201–38.

[87] EU. Directive (EU) 2018/844 of the European Parliament and of the Council of 30 May 2018. Official Journal of the European Union; 2018. Accessed: Dec. 21, 2022. [Online]. Available: https://eur-lex.europa.eu/legal-content/EN/TXT/?uri=celex%3A32018L0844.
[88] CIBSE. Guide A environmental design. London. Accessed: Feb. 12, 2023. [Online]. Available: https://www.cibse.org/knowledge-research/knowledge-portal/guide-a-environmental-design-2015; 2015.
[89] Fisk WJ. The ventilation problem in schools: literature review. Indoor Air Nov. 2017;27(6):1039–51. https://doi.org/10.1111/INA.12403.
[90] Stabile L, Dell'Isola M, Russi A, Massimo A, Buonanno G. The effect of natural ventilation strategy on indoor air quality in schools. Sci Total Environ Oct. 2017; 595:894–902. https://doi.org/10.1016/J.SCITOTENV.2017.03.048.
[91] Mundt E, Mathisen HM, Nielsen PV, Moser A. Ventilation effectiveness. Rehva; 2004.
[92] McLeod RS, Swainson M. Chronic overheating in low carbon urban developments in a temperate climate. Renew Sustain Energy Rev Jul. 2017;74:201–20. https://doi.org/10.1016/J.RSER.2016.09.106.
[93] Castro Dopico X, Ols S, Loré K, Karlsson Hedestam GB. Immunity to SARS-CoV-2 induced by infection or vaccination. J Intern Med Jan. 2022;291(1):32–50. https://doi.org/10.1111/JOIM.13372.
[94] Pilz S, Chakeri A, Ioannidis JPA, Richter L, Theiler-Schwetz V, Trummer C, et al. SARS-CoV-2 re-infection risk in Austria. Eur J Clin Invest Apr. 2021;51(4). https://doi.org/10.1111/ECI.13520. e13520.